Available online at www.sciencedirect.com
ScienceDirect
Journal of the European Ceramic Society 30 (2010) 3157–3165
www.elsevier.com/locate/jeurceramsoc

Low temperature preparation and electrical properties of sodium–potassium bismuth titanate lead-free piezoelectric thick films by screen printing

Haibo Zhang [a,b,c,*], Shenglin Jiang [a], Jianzhong Xiao [b], Koji Kajiyoshi [c]

[a] Department of Electronic Science and Technology, Huazhong University of Science and Technology, Wuhan 430074, China
[b] School of Materials Science and Engineering, State Key Laboratory of Material Processing and Die & Mould Technology, Huazhong University of Science and Technology, Wuhan 430074, China
[c] Research Laboratory of Hydrothermal Chemistry, Faculty of Science, Kochi University, Kochi 780-8520, Japan

Received 2 October 2009; received in revised form 21 June 2010; accepted 5 July 2010
Available online 31 July 2010

Abstract

Sodium–potassium bismuth titanate (NKBT) thick films with thickness of 40 μm were prepared by screen printing. To improve the homogeneity, the sintering aids were added into the pastes as a chemical liquid-phase doping method. The results show that the addition of Bi–Li sintering aids was beneficial for both the reduction of the sintering temperature and the improvement of the electrical performance of the thick films. The thick films containing 5 wt.% Bi–Li sintering aids demonstrated optimal dielectric properties with the maximum dielectric constant of 725 and minimum dielectric loss of 2.5%. Moreover, the NKBT thick films containing 3 wt.% Bi–Li sintering aids sintered at 950 °C exhibited the remanent polarization of 19.6 μC/cm^2, room-temperature pyroelectric coefficient of 1.56×10^{-4} C/(m^2 °C), figure of merit for specific detectivity of 0.48×10^{-5} Pa$^{-0.5}$, and effective longitudinal piezoelectric coefficient of 88 pm/V, which are comparable to that of the high-temperature sintered thick films without sintering aids.

Keywords: Ferroelectric properties; Pyroelectric properties; Piezoelectric properties; Potassium–sodium bismuth titanate; Thick films; Low-temperature sintering

1. Introduction

Bismuth sodium titanate, $(Bi_{0.5}Na_{0.5})TiO_3$ (NBT), is considered to be an excellent candidate as a key lead-free piezoelectric material because NBT is strongly ferroelectric with relatively large remanent polarization, $P_r = 38$ μC/cm^2, the strong ferroelectric performance of NBT ceramics is attributed to $(Bi_{0.5}Na_{0.5})^{2+}$ ions, especially Bi^{3+} ions, of A site on perovskite structure (ABO_3).[1,2] However, the NBT ceramics have a drawback of high conductivity and high coercive field, E_c, which make it difficult to be poled. In order to solve this problem and further improve its properties, some modifications on NBT composition have been performed. Nagata et al.[3] firstly reported that the piezoelectric properties of NBT ceramics modified with $Bi_{0.5}K_{0.5}TiO_3$–$BaTiO_3$ (KBT–BT) showed significant improved dielectric and piezoelectric properties. Elkechai et al.[4] firstly demonstrated the enhanced dielectric and piezoelectric properties of $Bi_{0.5}K_{0.5}TiO_3$ modified NBT ceramics. Recently, Sasaki et al.[5] have also reported a NBT–KBT solid solution ceramics show relatively high piezoelectric coefficient, $d_{33} = 151$ pC/N and $d_{31} = 46.9$ pC/N. They attributed the improvement of dielectric and piezoelectric properties for NBT ceramics modified with $Bi_{0.5}K_{0.5}TiO_3$ (KBT) to the corresponding rhombohedral tetragonal morphotropic phase boundary (MPB)[5–7] structures in solid solution. However, to the best of our knowledge, besides only several attempts at the fabrication of lead-free thin films, all most all of the studies about lead-free piezoelectric materials are limited in bulk ceramics. There is a dearth of reports on the investigation of the lead-free piezoelectric thick or thin films.

Recently, piezoelectric thick films with thickness in the range of 10–100 μm have received considerable attention for potential applications in the actuation of active structures in microelectromechanical system (MEMS).[8] They have been widely applied to micropumps, accelerometers, ultrasonic motors, resonators, elastic wave sensors microfluidic separators, high

* Corresponding author at: Research Laboratory of Hydrothermal Chemistry, Faculty of Science, Kochi University, 2-5-1 Akebono-cho, Kochi 780-8520, Japan. Tel.: +81 88 844 8350; fax: +81 88 844 8362.
E-mail address: changhb@gmail.com (H. Zhang).

0955-2219/$ – see front matter © 2010 Elsevier Ltd. All rights reserved.
doi:10.1016/j.jeurceramsoc.2010.07.012

frequency transducers, and pyroelectric thick film sensors, because they possesses the merits such as larger displacement and quick response, high frequency, light weight, and low power consumption.[9] Most recently, Kok and White[10] reported the research on screen-printed free-standing PZT thick films for energy harvesting, and their results showed the maximum output power of the thick film cantilevers is about 40 μW. However, the traditional thin-film processing, such as sol–gel, sputtering, physical vapour deposition, chemical vapour deposition, and pulsed laser deposition are not practical due to the slow deposition rates and high levels of stress generated during processing which can lead to cracking of the film. The thick-films technologies filled the gap between bulk ceramics and thin films. Many studies have been reported on the preparation of piezoelectric thick films by screen printing, tape casting, composite sol–gel, electrophoretic deposition, and aerosol deposition.[8] Among these methods, the screen printing technology has an advantage in that it enables low-cost fabrication of a device and device array in desired pattern without a photolithography. Torah et al.[11] have reported the research on screen-printing processing and properties PZT thick films, and described that improving the characteristics of the thick films by optimizing the powder milling process. The results have shown that the milling process can increase the homogeneity of the paste and improve the consistency of the thick-film prints. Recently, we have prepared NKBT lead-free piezoelectric thick films by screen printing, the high remanent polarization and longitudinal effective piezoelectric coefficient $d_{33\text{eff}}$ up to 28.3 μC/cm^2 and 109 pm/V have been obtained,[12] and we also produced NKBT lead-free thick films by using a combination of screen printing and subsequent infiltration of corresponding composite sol.[13] Most recently,[14] we prepared MnO doped NKBT thick films with thickness about 40 μm using screen printing on Pt electroded alumina substrates. The strong pyroelectric coefficient of 3.8×10^{-4} C/(m^2 °C) was observed in 1.0 mol% MnO doped thick films and the calculated figure of merit for specific detectivity reaches as high as 1.1×10^{-5} Pa$^{-0.5}$, which is comparable to that of the commonly used lead based materials. However, the firing temperature of the screen-printed NKBT thick films was higher than 1100 °C. The reaction layers, which deteriorate dielectric and piezoelectric properties, were formed at the interface between the substrates and NKBT piezoelectric layers when the thick films were fired at such high temperatures. In order to prevent these phenomena, densification must be carried out a low-temperature sintering for NKBT thick films.

The general approaches of low-temperature processing for piezoelectric ceramics or thick films are based on the addition of relatively low-melting oxide powders to the piezoelectric powders. The low-melting oxide additions for piezoelectric ceramics previously reported in the literatures include silicate glasses, Li_2O, $LiCO_3$, Bi_2O_3, and $BiFeO_3$.[15–17] Most recently, several publications described the processing of piezoelectric thick films prepared by screen printing with the addition of sintering aids. Thiele et al.[18] prepared lead zirconate titanate (PZT) piezoelectric thick films on silicon substrates by screen printing with the addition of B_2O_3–Bi_2O_3–CdO powders as sintering aids. The PZT thick films sintered at 900 °C for 1 h exhibit relative permittivity of 970, remanent polarization of 20 μC/cm^2, coercive field of 30 kV/cm, and weak-field piezoelectric coefficient d_{33} of 110 pm/V. Chen et al.[19] added a mixture of Li_2CO_3 and Bi_2O_3 powders as a sintering aid to the PZT-based pastes, and the films were fired at 850 °C atop a Ti/Pt bottom electrode sputtered onto silicon. Koch et al.[20] reported on the development of a PZT micropump on silicon substrates using gold cermet electrodes. The maximum d_{33} value measured for these films, which contained a borosilicate glass as sintering aid, was 173 pC/N. So far, to the best of our knowledge, we found almost all the sintering aids were added in piezoelectric ceramic powders or paste ink of thick films as solid-state powders.

However, mechanical mixing of the piezoelectric ceramic powders with the solid-state sintering aids usually results in a significant non-homogeneity in the distribution of the sintering aids in the mixture. The non-homogeneity leads to a non-uniform distribution of the liquid-phase sintering aids in the heating process, which will deteriorate the electrical properties of the piezoelectric thick films. Recently, Yao et al.[21] reported that 30 μm thick PZT films were deposited onto Pt-coated silicon wafers by a screen-printing process using the ink pastes containing the chemical liquid-phase sintering aids. These liquid-phase sintering aids were prepared from lithium ethoxide and bismuth nitrate pentahydrate. The sintering temperature of the PZT thick films was reduced to 925 °C.[21] Compared with bulk ceramics, the non-homogeneity is particularly serious for thick films because in order to minimize the reaction between the piezoelectric layer and the substrate, the subsequent high processing temperature and long processing time are not possible for sintering of thick films.

In the present study, we employed Bi_2O_3–Li_2O as the sintering aids to prepare NKBT thick films on Pt-coated alumina substrates by screen printing. Moreover, we expect to the Bi–Li sintering aids not only reduce the sintering temperature but also compensate the vacancies by the product of $(Bi_{0.5}Li_{0.5})^{2+}$ ions. On the other hand, in order to improve the homogeneity of the sintering aids introduced in NKBT pastes, the Bi–Li chemical liquid-phase sintering aids prepared from lithium ethoxide and bismuth nitrate pentahydrate were used to replace the commonly used sintering aids of Bi_2O_3–Li_2O solid powders. Furthermore, the microstructure, dielectric, ferroelectric and piezoelectric properties of the thick films were characterized. The mechanism of the improvement of the performance for NKBT thick films added with Bi–Li chemical liquid-phase was carefully discussed.

2. Experimental procedure

2.1. Preparation of NKBT thick films

A conventional solid-state reaction method was used to prepare the NKBT ceramic powders. Commercially available reagent grade metal oxide and carbonate powders TiO_2, Bi_2O_3, Na_2CO_3 and K_2CO_3 mixed according to chemical formula $Bi_{0.5}(Na_{0.82}K_{0.18})_{0.5}TiO_3$. These oxide and carbonate powders were mixed in ethanol and ball milled for 24 h. After calcining at 850 °C for 4 h, the powder mix was again ball milled

with the liquid-phase sintering aids for 48 h with the addition of ethanol. The liquid-phase sintering aids of Bi–Li and B–Si precursor solutions were prepared from lithium ethoxide and bismuth nitrate pentahydrate as well as boron trihydroxide and potassium silicate, respectively. The sintering aids were added into the NKBT ceramic powders with the weight ratio of 0, 1, 3, 5 and 7 wt.%. After the second ball milling procedure, the ground ceramic powders were dried at 60 °C for 24 h. The ground NKBT powder was ball milled for 4 h with the addition of 20–40 wt.% of organic vehicle. The organic vehicle usually consists of a binder (ethyl cellulose), a solvent (α-terpineol), a plasticizer (polyethylene glycol) and a dispersing agent (butoxyethoxyethyl acetate). After the third ball milling, the viscosity of the prepared screen-printable pastes was measured by viscosimeter and adjusted in the range 20–80 Pa s for shear rate 18^{-1} s. NKBT layers were screen-printed with a 320 mesh screen mask on 96% alumina substrates (20 mm × 15 mm × 0.5 mm), which were firstly electroded with an Pt paste. In order to fire the organic vehicle the layers precalcined at 550 °C for 5 min with a heating rate of 180 °C/min in rapid thermal processor (RTP). The processes from printing to firing were repeated seven times to obtain about 40 μm thick lead-free NKBT films. The detailed processing has been reported in our previous work.[18] The final firing of the piezoelectric thick films was performed at 850–1150 °C for 30 min in air.

2.2. Measurement

TG and DTA analysis for the dried NKBT screen pastes were carried out with Pyris Diamond TG/DTA thermogravimeter (Perkin-Elmer Instruments, USA) in dynamic nitrogen atmosphere and at a heating rate of 10 °C/min. The microstructures and the cross-section of the thick films were examined by field-emission scanning electron microscopy (FE-SEM, Sirion 200, FEI, USA) equipped with an energy dispersive X-ray analysis (EDX, EDAX Genenis-4000, USA) operated at 20 kV. NKBT thick film density was measured from its weight and volume. The film weight was obtained from the sample weight by subtracting the weight of the substrate, and the film volume was obtained from the surface shape of the film. The film thickness was achieved using Form Talysurf Series 2 profilometer (Rank Taylor Hobson Ltd.). The relative density of the film was calculated based on the pure NKBT, and the influence of sintering aids on the theoretical density was not taken into account.

For dielectric, ferroelectric, pyroelectric, and piezoelectric measurements, platinum top electrodes with diameters of 0.8 mm and thickness of 0.3 μm were sputtered onto the sintered NKBT layers. A dc power supply and a KEITHLEY 6517 electrometer with high input impedance (Keithley Instruments Inc., USA) was used to measure the leakage currents. The NKBT thick films were poled using 100–600 kV/cm applied field at 100 °C for 10 min in silicone oil. The films are short-circuited for 24 h after poling in order to allow the release of excess charges injected during the poling process. Moreover, in order to avoid confusing loosely bound space charge with true polarization, the temperature cycled several times before the record of pyroelectric current of the thick films. The pyroelectric current, i_p, was measured by a KEITHLEY 6485 Picoammeter (Keithley Instruments Inc., USA) while raising the temperature at a constant rate of 1.0 °C/min over the 20–80 °C range using a programmed temperature control system.[26] Dielectric performance measurements were performed using an LF impedance analyzer (Model HP 4192A, Hewlett-Packard, USA), a modified Sawyer–Tower circuit for ferroelectric hysteresis measurements, and a dual-beam laser interferometer for the longitudinal piezoelectric charge coefficient (d_{33eff}) measurements.

3. Results and discussion

TG and DTA analyses were performed to determine the vapourization temperature of various organic binders and melting temperature of sintering aids after screen printing of NKBT pastes on alumina substrates. As shown in Fig. 1, in the range of 30–1000 °C, the total weight loss of 16% can be observed from TG curve. In the DTA curve, two exothermic peaks appear at 355.3 and 403 °C, which resulting from the decomposition or combustion of ethyl cellulose and α-terpineol, respectively. This indicates that the most of the organic vehicle has been burned at around 450 °C, thus it is necessary to keep the presintering temperature of the NKBT thick films at 450 °C. The other two exothermic peaks located at 497.4 and 619.9 °C were attributed to the combustion of organic residues. The endothermic peaks were observed at 693.2 and 825.8 °C due to the melting of sintering aids added in screen pastes. The heat treatment at a temperature of 850 °C for 30 min was concluded to be sufficient for the melting of sintering aids and forming the liquid phases in NKBT thick films.

Fig. 2 shows the XRD patterns of NKBT thick films (sintered at 950 °C) added with 3 wt.% Bi–Li and 3 wt.% B–Si sintering aids. In order to determine the phase structure, fine scanning XRD patterns in the selected 2θ ranges of 45–48° and 55–61° of NKBT thick films with Bi–Li and B–Si sintering aids are shown in Fig. 2(b). It can be seen that the rhombohedral symmetry and tetragonal symmetry of the NKBT thick films at room temperature are characterized by a (0 0 2)/(2 0 0) peak splitting near 46° and a (2 1 1)/(1 1 2) peak splitting near 58°, respectively.[22] The existence of the MPB between rhombohedral NBT and tetragonal KBT phases of the NKBT thick films is beneficial to the

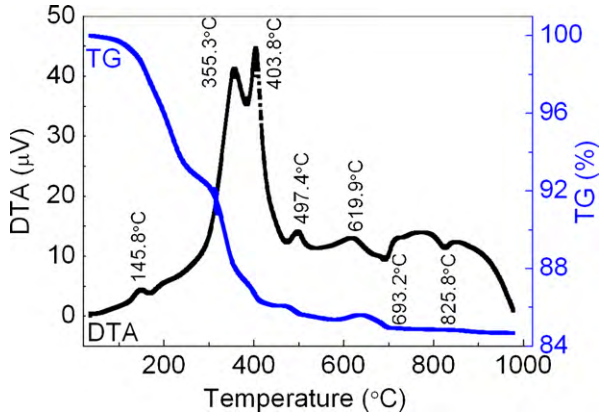

Fig. 1. TG-DTA curves of the dried NKBT screen pasts.

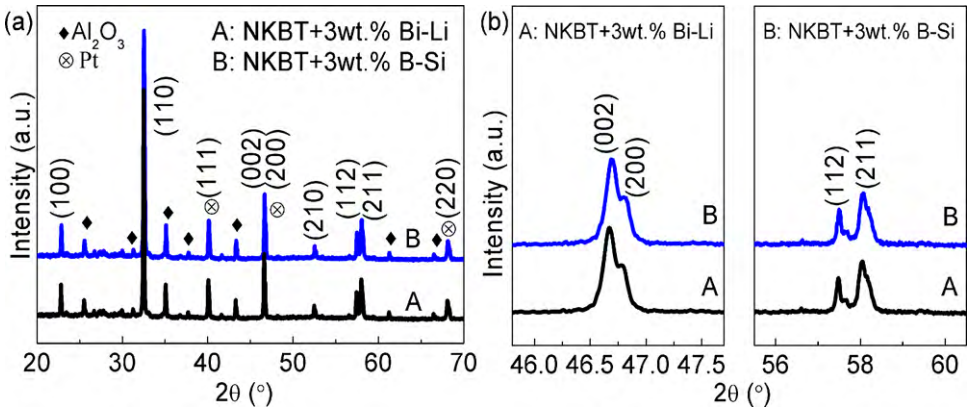

Fig. 2. XRD patterns in the 2θ range of 20–70° (a) and the fine scanning XRD patterns in the selected 2θ ranges of 45–48° and 55–61° (b) of NKBT thick films with Bi–Li and B–Si sintering aids.

high piezoelectric and ferroelectric properties. Furthermore, the two samples present the pure perovskite structures and the coexistence of rhombohedral and tetragonal phases, which indicates that addition of sintering aids does not change the crystalline structures and no second phase was observed. The Bi^{3+}, K^{+} and Li^{+} ions diffused into the NKBT lattices to form a solid solution with a pure perovskite structure. Moreover, the results of XRD diffraction also imply that the relatively low sintering temperature of 950 °C does not change the pure perovskite crystalline structures of NKBT thick films. Compared with the conventional ceramic processing, the relative shorter time of the sintering of the NKBT thick films is believed to be responsible for the reduction of the deviation of the compositional change.

In order to compare the performance of different sintering aids, we measured the density of NKBT thick films added with Bi–Li and B–Si solutions as the sintering aids sintered at various temperatures. Fig. 3 shows the apparent density and relative density as a function of sintering temperature for NKBT thick films with 3 wt.% of sintering aids Bi–Li and B–Si. The insert figure shows *P–E* hysteresis loops of the corresponding NKBT thick films sintered at 950 °C for 30 min, which implies the excellent ferroelectric properties can be obtained in low-temperature processed thick films containing sintering aids. It can be seen

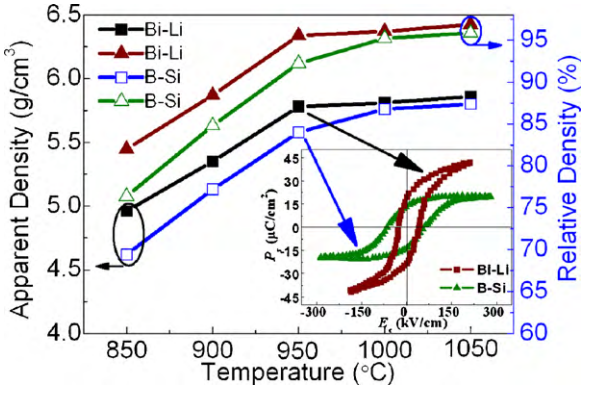

Fig. 3. Apparent density and relative density as a function of sintering temperature for NKBT thick films with different sintering aids. The insert figure shows *P–E* hysteresis loops of the corresponding NKBT thick films sintered at 950 °C for 30 min.

that the NKBT thick films with 3 wt.% Bi–Li sintered at 950 °C exhibited high relative density of 95.54%, which indicates that the sintering temperature of NKBT thick films was decreased from 1150 to 950 °C. Otherwise, with the addition of 3 wt.% sintering aids of B–Si the NKBT fired at 950 °C exhibited relative density of 92.23%. As the temperature increases, the liquid phases resulting from sintering aids along solid-state boundaries accelerated the grain growth and densification of the NKBT thick films. Meanwhile, compared with B–Si sintering aids, the Bi–Li sintering aids added as sintering aids were more effective to increase the density of the NKBT thick films sintered at relative low temperature.

However, the secondary or grain boundary phases deriving from the sintering aids somewhat deteriorate the properties of NKBT thick films. In order to determine which sintering aid caused less deterioration in performance of NKBT thick films. We investigated the ferroelectric properties of NKBT thick films added with B–Si and Bi–Li sintered at various temperatures. The remanent polarization as a function of sintering temperature for NKBT thick films with different sintering aids is shown in Fig. 4. As the temperature increase, all of the samples exhibited the increasing remanent polarization, which was attributed to the increasing density of the NKBT thick films. Moreover, the NKBT thick films added with 3 wt.% Bi–Li exhibited optimal ferroelectric properties with the maximum

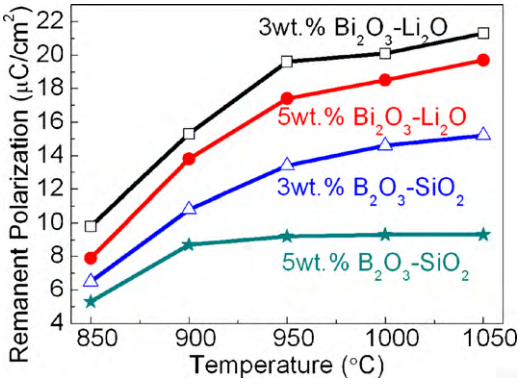

Fig. 4. Remanent polarization as a function of sintering temperature for NKBT thick films with different sintering aids.

remanent polarization of 19.6 μC/cm^2 and minimum coercive field of 57.3 kV/cm. However, the NKBT thick films added with 5 wt.% Bi–Li showed a comparatively lower remanent polarization of 17.4 μC/cm^2. This result implies that although addition of 5 wt.% Bi–Li as sintering aids can further increase the density of the NKBT thick films, part of the excessive sintering aids remaining at the grain boundaries can deteriorate the ferroelectric properties of the films. Because the sintering aids exist in NKBT thick films as non-ferroelectric phases, the remanent polarization of the films sintered at the same temperature decreases with the increasing content of sintering aid from 3 to 5 wt.%. Thus, we can conclude that a small amount sintering aids added in NKBT thick films can increase the density and improve the performances, but the excess sintering aids inhibit the grain growth and deteriorate the performances.

Meanwhile, it can be seen that the reduction of remanent polarization of the thick films containing Bi–Li is less than that of the thick films added with B–Si when the content of the sintering aids increased from 3 to 5 wt.%. Even though the B–Si precursor (potassium silicate) containing K^+ which can compensate the vacancies of both Na^+ and K^+ in the thick film, it cannot change the pure perovskite structure. The significant difference of the effect of the two sintering aids on the properties of NKBT thick films was ascribed to two aspects. Firstly, Bi_2O_3 can compensate the Bi vacancies resulting from the evaporation of bismuth oxide during sintering.[23] Secondly, in the prophase of sintering, Li_2O melted to form liquid phase which accelerate the densification of the films, and then the Li ions entered the NKBT perovskite lattices acted as acceptor dopants in the telophase of the sintering. It is known that Bi^{3+}, Na^+ and K^+ ions could leave NKBT thick films to form vacancies in the lattice during high temperature. These vacancies can be compensated by the product of $(Bi_{0.5}Li_{0.5})^{2+}$ ions and formed a new chemical formula of $(Na_{0.82}K_{0.18})_{0.5}Bi_{0.5}TiO_3$–$(Li_{0.5}Bi_{0.5})TiO_3$ (NKLBT) thick film. The XRD patterns as shown in Fig. 2 present that the NKBT thick films have pure perovskite structure and no second phases can be detected, indicating that Li^+ ions diffuse into the NKBT lattices. Moreover, the partial substitution of Li^+ in A site could lower the coercive field and increase the remanent polarization.[24] Sung et al.[25] also reported that Li and K doping in NBT ceramics could enhance the piezoelectric properties due to the tetragonality optimized by Li addition. In present study, the Bi–Li with dual effect of the sintering aids on the NKBT thick films, significantly reduced the sintering temperature and improved the performance of the thick films simultaneously. Therefore, we choose Bi–Li liquid sintering aids to lower the sintering temperature of NKBT thick films, and the following text will discuss the influence of the Bi–Li aids on the microstructure and electronic performances of NKBT thick films.

The different performances of the NKBT thick films added with different amount of sintering aids were related to the different microstructures of the films. Fig. 5 demonstrates the surface micrographs of the NKBT thick films with 3 wt.% (b), 5 wt.%, 7 wt.% and without Bi–Li as sintering aids sintered at 950 °C. The NKBT thick films without sintering aids showed a porous structure and informal grain size as shown in Fig. 5(a), and the abnormal grain growth can be observed in the NKBT thick films added sintering aids.[26] The introduction of proper amount of sintering aids favored considerably improvement the densification of the films resulting from the decrease of interface energy of grain boundaries due to presence of liquid phases. The excess sintering aids aggregated at the grain boundaries as a second phase had a substantial damaging effect on the final electrical and physical properties of the thick films as shown in Fig. 5(d).

The interfacial layer is believed to be the intrinsic dead layer (low-dielectric layer) due to the diffusion kinetics caused by the undesirable reaction between the NKBT thick film and substrate.[27] Although the double screen-printed Pt electrode layer with relative high compact structure on alumina substrate to prevent the diffusion, the interfacial layer can be observed from the SEM micrograph of the cross-section of the NKBT thick film. In order to estimate the thickness of the interfacial layer, the element linear energy dispersive X-ray spectroscopy (EDAX) scanning was employed to investigate the cross-section of the films. Fig. 6 shows the SEM micrographs and element linear EDAX scanning of the cross-section of the NKBT thick films. It can be seen from Fig. 6(b) that there was an interfacial zone where the intensity of the Ti, Bi, K, and Na element decreases slowly at the interface of the NKBT films and the substrate. This 1.1–1.6 μm thick interfacial layer is the low-dielectric layer resulting from the reaction between the NKBT film and the substrate.[28] However, the interface between the thick film and Pt/Al_2O_3 substrate layer was abrupt. Compared with the thickness of the thick film, the thickness of the interfacial layer is relatively small. Moreover, compared with the ferroelectric thick film prepared by screen printing sintering at high temperature[29] the NKBT thick film sintered at 950 °C only presented very slight interdiffusion and reaction between thick film and Pt/Al_2O_3 substrate layer. The thickness of the interfacial layer was significantly reduced by the low-temperature sintering process due to the addition of the Bi–Li sintering aids, which was beneficial to improvement of the electrical properties of the thick films.[8]

Fig. 7 illustrates the relative dielectric constant, ε_r, and dielectric loss, $tg\delta$, as a function of sintering aid contents for NKBT thick films sintered at 950 °C. The NKBT thick films added 5 wt.% Bi–Li sintering aids demonstrate optimal dielectric properties with the maximum dielectric constant of 725 and minimum dielectric loss of 2.5% as shown in Fig. 7(a), which is consistent with the results of microstructure. The reduction of porosity and the increment of densification of the NKBT thick films with 5 wt.% sintering aids was responsible for the improvement of dielectric performances. Even though the NKBT thick films containing 5 wt.% Bi–Li sintering aids exhibit slightly higher room-temperature dielectric constant than the films containing 3 wt.% Bi–Li sintering aids. The NKBT thick films containing 3 wt.% Bi–Li sintering aids still show better ferroelectric and piezoelectric properties, which is in perfect concordance with the results shown in Fig. 4. This is caused by that part of the excess sintering aids remaining at the grain boundaries deteriorate the ferroelectric and piezoelectric properties of the NKBT thick films as the content of sintering aid increasing from 3 to 5 wt.%. Therefore, in the present study, the temperature dependence of dielectric properties were measured

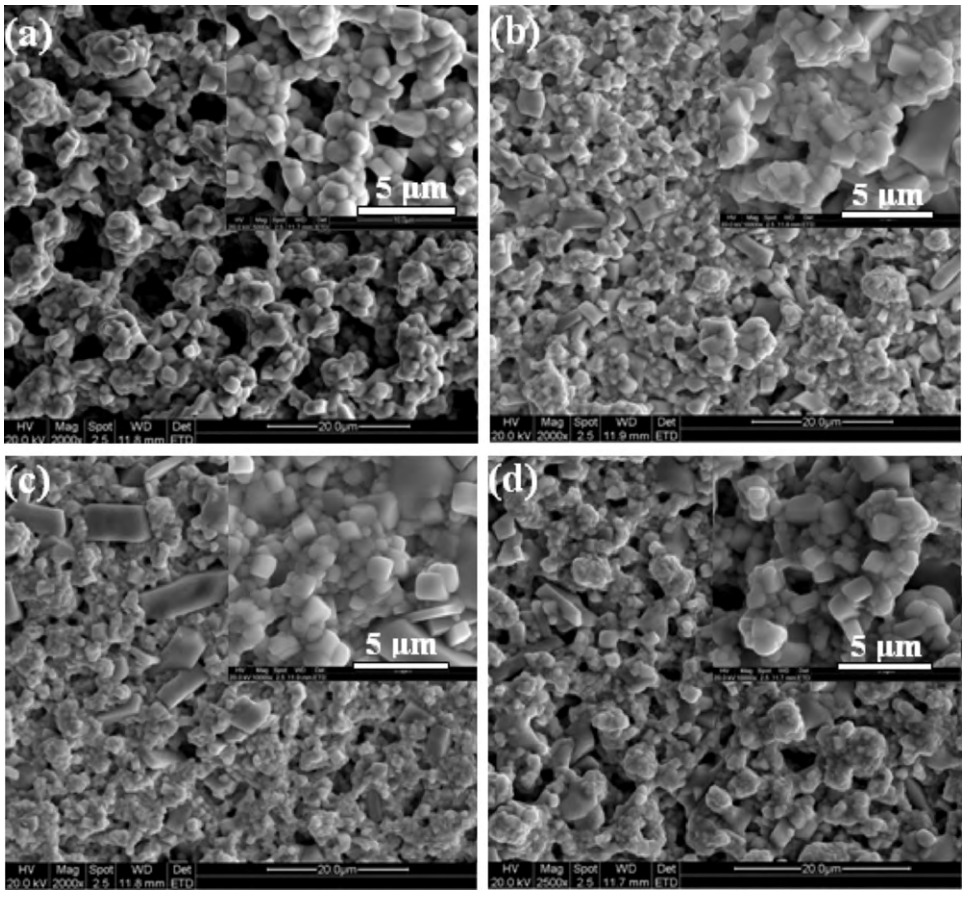

Fig. 5. SEM micrographs of the NKBT thick films with sintering aids of 0 wt.% (a), 3 wt.% (b), 5 wt.% (c), and 7 wt.% (d).

on the NKBT thick films added with 3 wt.% Bi–Li sintering aids. Fig. 7(b) shows the dielectric constant and dielectric loss as functions of temperature for NKBT thick films containing 3 wt.% sintering aids sintered at 950 °C for 0.5 h at 1, 10 and 100 kHz. It is known that the dielectric constant and dielectric loss of NBT based ceramics depends on frequency, as there is a hump between room temperature and 230 °C as well as a dispersion of the dielectric constant at temperatures over 300 °C.[5] The local maximum dielectric loss and dielectric constant locate at 150 °C (T_f) and 350 °C (T_m), respectively. A phase transition from the ferroelectric to the antiferroelectric phase for NKBT thick films is observed at about 150 °C, which is in line with a previous report.[6] Although some literatures proposed that this is not a ferroelectric to antiferroelectric phase transition.[30] In recent years, more and more researchers found the antiferroelectric phase in NBT based materials at the temperature higher than that transition. Dul'kin et al.[31] detected ferroelectric to antiferroelectric phase transation in NBT based single crystals by acoustic emission. Moreover, using TEM and SAED measurement, Dorcet and Trolliard[32,33] believed ferroelectric to antiferroelectric and

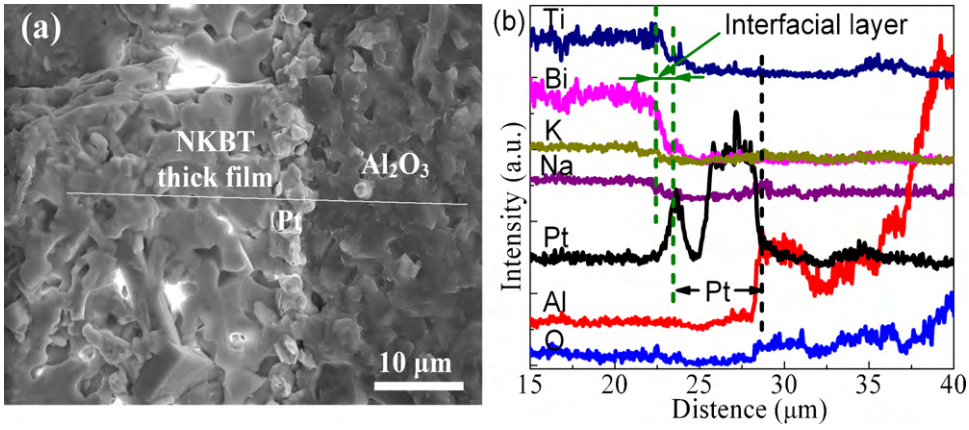

Fig. 6. SEM micrographs (a) and element linear EDAX scanning (b) of the cross-section of the NKBT thick films.

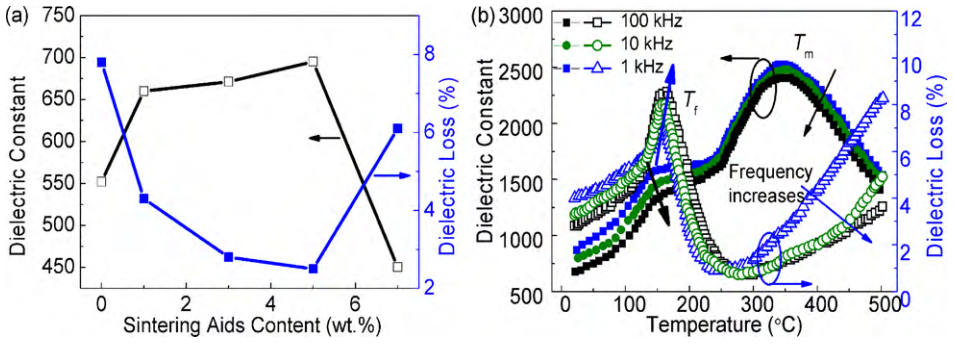

Fig. 7. (a) Dielectric constant and dielectric loss as a function of sintering aids content for NKBT thick films sintering at 950 °C and (b) temperature dependence of the dielectric constant and dielectric loss of NKBT thick film with 3 wt.% sintering aids at frequencies of 1, 10 and 100 kHz.

antiferroelectric to paraelectric transitions occurred near 200 and 320 °C, respectively.

In addition, the significant increase of the dielectric loss at high temperature and low frequencies is significant of space charge polarization and associated ionic conductivity. It also can be found that the temperature of local maximum (T_f) of both dielectric constant and dielectric loss slightly shifted to higher temperature as frequency increases. The value of dielectric constant in the local maximum (T_m) decreases and its temperature, T_m, shifted upward with increasing frequency in a way similar to that observed for typical relaxor materials. This typical relaxior behavior has been observed in many studies about NBT based materials.[23,24] As Na^+ and Bi^{3+} cations are randomly distributed in the 12-fold coordination site, the relaxation behaviour would reasonably attributed to some disorder induced by the presence of K^+ as well as some A site vacancies due to the sintering process. Moreover, the added Bi–Li sintering aids may block the movement of Na^+ and Bi^{3+} cations due to the change in the space charge polarization.

Fig. 8(a) describes the temperature dependence of pyroelectric coefficients of NKBT thick films added with 3 wt.% Bi–Li sintering aids and pure NKBT thick films in the range of 20–80 °C. In the temperature range between 20 and 80 °C, the pyroelectric coefficient of NKBT thick films containing 3 wt.% Bi–Li sintering aids was much larger than that of pure NKBT thick films at the same temperature. The room temperature (20 °C) pyroelectric coefficient of 1.56×10^{-4} C/(m^2 °C) was observed in NKBT thick films added with 3 wt.% sintering aids, resulting from the improvement of the ferroelectric performance and increase of the amplitude of dipole vibration with temperature. The figure of merit F_D for specific detectivity of pyroelectric IR sensors can be expressed by

$$F_D = \frac{p}{c_v\sqrt{\varepsilon_r\varepsilon_0 tg\delta}} \quad (1)$$

where the c_v is the volume specific heat, $c_v = 2.8$ J/(K cm^3) for NKBT ceramics.[34] According to the Eq. (1), the pyroelectric figure of merit is affected by the pyroelectric coefficient, dielectric constant, dielectric loss, and volume specific heat of the NKBT thick films.

As shown in Fig. 8(b), the maximum figure of merit for specific detectivity of NKBT thick films reached as high as 0.48×10^{-5} Pa$^{-0.5}$ at 20 °C, which was comparable to that of screen-printed lead zirconate titanate/uranium doped lead magnesium niobate–lead zirconate titanate (PZT/PMNZTU) thick films fabricated by Dorey and Whatmore.[8] Note that the values of F_D were calculated from the data of the dielectric properties measured in 100 kHz. Because the infrared devices are commonly used in low frequency (<100 Hz), The calculated F_D in low frequency (50 Hz) is 0.51×10^{-5} Pa$^{-0.5}$, which is about half of the value of 1.01×10^{-5} Pa$^{-0.5}$ of the F_D calculated by Dorey and Whatmore in 30 Hz.[35] The detectivity figure of merit significantly influenced by the frequency because the dielectric constant and the dielectric loss changed with the frequency.

The effective longitudinal piezoelectric coefficient d_{33eff} as a function of dc electric field is shown in Fig. 9. The insert figure

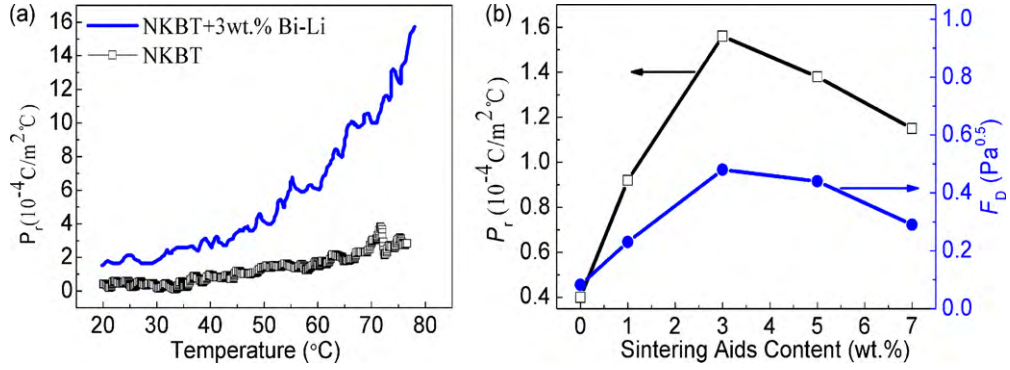

Fig. 8. (a) Temperature dependence of pyroelectric coefficient of NKBT thick films added with 3 wt.% sintering aids and pure NKBT thick films in the range of 20–80 °C and (b) room temperature detectivity figure of merit as a function of sintering aids content for NKBT thick films sintering at 950 °C.

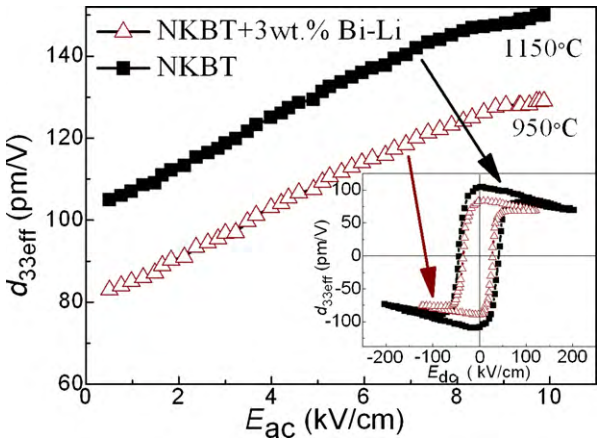

Fig. 9. Longitudinal piezoelectric coefficient d_{33eff} measured as a function of driving electric field amplitude for the NKBT thick film with and without sintering aids. The insert figure shows piezoelectric coefficient d_{33eff} as a function of dc electric field for the thick films driving at 0.1 kV/cm.

shows piezoelectric coefficient d_{33eff} as a function of dc electric field for the thick films driving at 0.1 kV/cm. The effective longitudinal piezoelectric coefficient was found to slightly decrease under the high dc bias E_{dc}. This typical behavior of the NKBT thick films came from the decrease of the number of domain walls, which reduces the extrinsic contribution to piezoelectric coefficient.[36] The value of d_{33eff} of the NKBT thick film without sintering aids sintered at 1150 °C reached high values of 109 pm/V. The NKBT thick films with 3 wt.% sintering aids of Bi–Li sintered at 950 °C also exhibited as high d_{33eff} as 88 pm/V. The strong field dependence of effective d_{33eff} at different dc fields suggests active contribution of non-180° domain walls in the thick film.[18] The active contribution of non-180° domain walls in NKBT thick films with 3 wt.% Bi–Li sintering aid indicates that relatively high concentration of the sintering aids did not inhibit the displacement of domain walls. The linear dependence of the longitudinal piezoelectric coefficient on the applied ac electric field indicates domain wall contributions to the polarization and piezoelectric strain, as observed in bulk ceramics.[37] Comparable properties of the NKBT thick film with and without sintering aids further indicate that the decrease in the properties of the films with respect to the NKBT bulk ceramics is mainly due to the presence of additives.

4. Conclusions

NKBT lead-free thick films with thickness of 40 μm have been prepared using screen printing on Pt electroded alumina substrates. The liquid-phase sintering aids of Bi–Li precursor solutions which were prepared from lithium ethoxide and bismuth nitrate pentahydrate were added into screen pastes to achieve homogeneous distribution in the NKBT thick films. The Bi_2O_3–Li_2O powders as the commonly used sintering aids were replaced by lithium ethoxide and bismuth nitrate pentahydrate solutions. The Bi–Li liquid-phase sintering aids added into the screen paste with improved homogeneity not only can decrease the sintering temperature of thick films, but also can modify electrical properties of NKBT as dopants. Our results show that the NKBT thick films with 3 wt.% Bi–Li sintering aids sintered at 950 °C exhibiting the dielectric constant of 671 and dielectric loss of 3.8%, strong remanent polarization of 19.6 μC/cm^2 and high effective longitudinal d_{33eff} piezoelectric coefficient of 88 pm/V in room temperature. Moreover, the room-temperature pyroelectric coefficient of 1.56×10^{-4} C/(m^2 °C) was observed in NKBT thick films containing 3 wt.% sintering aids, resulting from the improvement of the ferroelectric performance and increase of the amplitude of dipole vibration with temperature. The maximum figure of merit for specific detectivity of NKBT thick films reaches as high as 0.48×10^{-5} Pa$^{-0.5}$ at 20 °C, which is comparable to that of screen-printed lead based ferroelectric thick films. The thick films are expected to be a new and promising candidate for applications in lead-free piezoelectric microactuators and uncooled infrared detectors.

Acknowledgements

This research was partially supported by China Postdoctoral Science Foundation (No. 20090460933), national High Technology Research and Development Program of China (No. 2007AA03Z120), and the National Natural Science Foundation of China (No. 60777043).

References

1. Nagata H, Takenaka T. Lead-free piezoelectric ceramics of $(Bi_{1/2}Na_{1/2})TiO_3$–1/2(Bi_2O_3 Sc_2O_3) system. *Jpn J Appl Phys Part I* 1997;**36**:6055–7.
2. Takenaka T, Maruyama K-i, Sakata K. $(Bi_{1/2}$ $Na_{1/2})TiO_3$–$BaTiO_3$ system for lead-free piezoelectric ceramics. *Jpn J Appl Phys Part I* 1991;**30**:2236–9.
3. Nagata H, Yoshida M, Makiuchi Y, Takenaka T. Large piezoelectric constant and high curie temperature of lead-free piezoelectric ceramic ternary system based on bismuth sodium titanate–bismuth potassium titanate–barium titanate near the morphotropic phase boundary. *Jpn J Appl Phys* 2003;**42**:7401–3.
4. Elkechai O, Manier M, Mercurio JP. $Na_{0.5}Bi_{0.5}TiO_3$–$K_{0.5}Bi_0$ (NBT–KBT) system: a structural and electrical study. *Phys Stat Solidi A: Appl Res* 1996;**157**:499–506.
5. Sasaki A, Chiba T, Mamiya Y, Otsuki E. Dielectric and piezoelectric properties of $(Bi_{0.5}Na_{0.5})TiO_3$–$(Bi_{0.5}K_{0.5})TiO_3$ systems. *Jpn J Appl Phys Part I* 1999;**38**:5564–7.
6. Isupov VA. Ferroelectric $Na_{0.5}Bi_{0.5}TiO_3$ and $K_{0.5}Bi_{0.5}TiO_3$ perovskites and their solid solutions. *Ferroelectrics* 2005;**315**:123–47.
7. Yoshii K, Hiruma Y, Nagata H, Takenaka T. Electrical properties and depolarization temperature of $(Bi_{1/2}Na_{1/2})TiO_3$–$(Bi_{1/2}K_{1/2})TiO_3$ lead-free piezoelectric ceramics. *Jpn J Appl Phys Part I* 2006;**45**:4493–6.
8. Dorey RA, Whatmore RW. Electroceramic thick film fabrication for MEMS. *J Electroceram* 2004;**12**:19–32.
9. Torah RN, Beeby SP, Tudor MJ, White NM. Thick-film piezoceramics and devices. *J Electroceram* 2007;**19**:95–110.
10. Kok SL, White NM, Harris NR. Fabrication and characterization of free-standing thick-film piezoelectric cantilevers for energy harvesting. *Meas Sci Technol* 2009;**20**:124010.
11. Torah RN, Beeby SP, White NM. Improving the piezoelectric properties of thick-film PZT: the influence of paste composition, powder milling process and electrode material. *Sens Actuators A* 2004;**110**:378–84.
12. Zhang HB, Jiang SL, Zeng YK. Piezoelectric property in morphotropic phase boundary $Bi_{0.5}(Na_{0.82}K_{0.18})_{0.5}TiO_3$ lead free thick film deposited by screen printing. *Appl Phys Lett* 2008;**92**:152901.

13. Zhang HB, Jiang SL. Effect of repeated composite sol infiltrations on the dielectric and piezoelectric properties of a $Bi_{0.5}(Na_{0.82}K_{0.18})_{0.5}TiO_3$ lead free thick film. *J Eur Ceram Soc* 2009;**29**:717–23.
14. Zhang HB, Jiang SL, Kajiyoshi K. Pyroelectric and dielectric properties of Mn modified $0.82Bi_{0.5}Na_{0.5}TiO_3$–$0.18Bi_{0.5}K_{0.5}TiO_3$ lead-free thick films. *J Am Ceram Soc* 2009;**92**:2147–50.
15. Tandon RP, Singh V, Singh R. Properties of low temperature sintered neodymium doped lead zirconate titanate ceramics. *J Mater Sci Lett* 1994;**13**:810–2.
16. Cheng S-Y, Fu S-L, Wei C-C. Low-temperature sintering of PZT ceramics. *Ceram Int* 1987;**13**:223–31.
17. Kaneko S, Dong D, Murakami K. Effect of simultaneous addition of $BiFeO_3$ and $Ba(Cu_{0.5}W_{0.5})O_3$ on lowering of sintering temperature of $Pb(Zr,Ti)O_3$ ceramics. *J Am Ceram Soc* 1998;**81**:1013–8.
18. Thiele ES, Damjanovic D, Setter N, Processing. Properties of screen-printed lead zirconate titanate piezoelectric thick films on electroded silicon. *J Am Ceram Soc* 2001;**84**:2863–8.
19. Chen HD, Udayakumar KR, Cross LE, Bernstein JJ, Niles LC. Dielectric, ferroelectric, and piezoelectric properties of lead zirconate titanate thick films on silicon substrates. *J Appl Phys* 1995;**77**:3349–53.
20. Koch M, Harris N, Maas R, Evans AGR, White NM, Brunnschweiler A. A novel micropump design with thick-film piezoelectric actuation. *Meas Sci Technol* 1997;**8**:49–57.
21. Yao K, He X, Xu Y, Chen M. Screen-printed piezoelectric ceramic thick films with sintering additives introduced through a liquid-phase approach. *Sens Actuators A* 2005;**118**:342–8.
22. Zhang YR, Li JF, Zhang BP. Enhancing electrical properties in NBT–KBT lead-free piezoelectric ceramics by optimizing sintering temperature. *J Am Ceram Soc* 2008;**91**:2716–9.
23. Wang XX, Tang XG, Kwok KW, Chan HLW, Choy CL. Effect of excess Bi_2O_3 on the electrical properties and microstructure of $(Bi_{1/2}Na_{1/2})TiO_3$ ceramics. *Appl Phys A: Mater* 2005;**80**:1071–5.
24. Lin D, Zheng Q, Xu C, Kwok KW. Structure electrical properties and temperature characteristics of $Bi_{0.5}Na_{0.5}TiO_3$–$Bi_{0.5}K_{0.5}TiO_3$–$Bi_{0.5}Li_{0.5}TiO_3$ lead-free piezoelectric ceramics. *Appl Phys A: Mater Sci Process* 2008;**93**:549–58.
25. Sung YS, Lee HM, Du W, Yeo HG, Lee SC, Cho JH, et al. Enhanced piezoelectric properties of $(Bi_{0.5}K_{0.5+x}Li_y)TiO_3$ ceramics by K nonstoichiometry and Li addition. *Appl Phys Lett* 2009;**94**:062901.
26. Zhou LJ, Zimmermann A, Zeng Y-P, Aldinger F. Effects of PbO content on the sintering behavior, microstructure, and properties of La-doped PZST antiferroelectric ceramics. *J Mater Sci: Mater Electron* 2004;**15**:145–51.
27. Holc J, Hrovat M, Kosec M. Interactions between alumina and PLZT thick films. *Mater Res Bull* 1999;**34**:2271–8.
28. Bersani M, Morten B, Prudenziati M, Gualtieri A. Interactions between lead oxide and ceramic substrates for thick film technology. *J Mater Res* 1997;**12**:501–8.
29. Futakuchi T, Nakamura Y, Adachi M. Preparation of $Ba(Ti,Zr)O_3$ thick films by screen printing. *Jpn J Appl Phys* 2002;**41**:6948–51.
30. Tai CW, Choy SH, Chan HLW. Ferroelectric domain morphology evolution and octahedral tilting in lead-free $(Bi_{1/2}Na_{1/2})TiO_3$–$(Bi_{1/2}K_{1/2})TiO_3$–$(Bi_{1/2}Li_{1/2})TiO_3$–$BaTiO_3$ ceramics at different temperatures. *J Am Ceram Soc* 2008;**91**:3335–41.
31. Dul'kin E, Mojaev E, Roth M, Greicius S, Granzow T. Detection of phase transitions in sodium bismuth titanate–barium titanate single crystals by acoustic emission. *Appl Phys Lett* 2008;**92**:012904.
32. Dorcet V, Trolliard G, Boullay P. Reinvestigation of phase transitions in $Na_{0.5}Bi_{0.5}TiO_3$ by TEM. Part I: First order rhombohedral to orthorhombic phase transition. *Chem Mater* 2008;**20**:5061–73.
33. Trolliard G, Dorcet V. Reinvestigation of phase transitions in $Na_{0.5}Bi_{0.5}TiO_3$ by TEM. Part II: Second order orthorhombic to tetragonal phase transition. *Chem Mater* 2008;**20**:5074–82.
34. Abe J, Kobune M, Nishimura T, Yazaw T, Nakai Y. Effects of manganese addition on pyroelectric properties of $(Bi_{0.5}Na_{0.5}TiO_3)_{0.94}(BaTiO_3)_{0.06}$ ceramics. *Integr Ferroelectr* 2006;**80**:87–95.
35. Dorey RA, Whatmore RW. Pyroelectric PZT/PMNZTU composite thick films. *J Eur Ceram Soc* 2005;**25**:2379–82.
36. Shvartsman VV, Pertsev NA, Herrero JM, Zaldo C, Kholkin AL. Nonlinear local piezoelectric deformation in ferroelectric thin films studied by scanning force microscopy. *J Appl Phys* 2005;**97**:1–11.
37. Damjanovic D. Stress and frequency dependence of the direct piezoelectric effect in ferroelectric ceramics. *J Appl Phys* 1997;**82**:1788–97.